Tracking Parameters of a Neural Mass Model: A Method to Provide Insight into the Mechanisms behind Seizure

R.S. Balson

February 21, 2013

1 Introduction

Aims

Estimate model parameters from a neural mass model of the hippocampus. Epilepsy is not well understood. Approximately one third of patients with epilepsy are refractory to treatment, and not much is understood about the mechanisms underlying seizures. In this paper, a new method to image aspects of the brain is introduced. This method involves the application of a well known neural mass model with a relatively new estimation technique. In particular, the estimation of physiologically relevant parameters from a neural mass model of the hippocampus (Wendling et al., 2002) is considered, using an unscented Kalman filter (Voss et al., 2004).

To improve the understanding of epilepsy and improve the outcome of epilepsy patients. By estimating the physiologically relevant parameters from the neural mass model of the hippocampus, it will be possible to image the changes occurring in the brain prior to seizure. This will be achieved by estimating model parameters based on electrographic recordings of seizures recorded from the hippocampus. Further, this method can be applied to determine the effect that treatment has on the physiological parameters. Imaging the brain in this manner will make it possible to titrate therapies that are patient specific and therefore more efficacious. For example, if it is observed that the model parameter describing inhibition decreases prior to seizure, a treatment that has the opposite effect on the model parameter can be determined and used on the specific patient.

How has this been achieved previously?

Introduction to neural mass model, freeman, jansen etc The original formulation of the neural mass model was in the early 1970's (Lopes da Silva et al., 1974; Freeman, 1963). The model was further developed in the mid 1990's. In this model, a cortical region of the brain is modeled as having a population of inhibitory and excitatory neurons, with the excitatory neurons being responsible for the production of the observed electrographic activity. This neural mass model was capable of replicating normal, or background, EEG as well as slow rhythmic activity, or alpha waves (Jansen and Rit, 1995). This description by Jansen and Rit was capable of replicating background and alpha rhythms observed in EEG by altering model parameters.

Inadequacy of jansen model and intro to the wendling model The model described by Jansen and Rit (1995) was shown to be capable of replicating other key features observed in EEG. However, the model was not able to replicate a key feature observed prior to seizure for recordings from the hippocampus, low amplitude high frequency EEG. A study performed by White et al. (2000) showed a possible reason for the models inability to replicate low amplitude high frequency EEG. They showed that within the hippocampus the inhibitory populations effect on excitatory

populations had two distinctly different propagation delays, and that both were significant for the reproduction of EEG. They hypothesised that the cause of the two different propagation delays were due to the location of the synapses connecting the inhibitory populations to the excitatory populations. With the longer propagation delay due to synapse connections far from the soma (peri-dendritic), and the shorter delay due to connections near the soma (peri-somatic). This effect was incorporated into the neural mass model by Wendling et al. (2002). In order to account for the two propagation delays observed the Wendling group described two different types of inhibitory populations. One fast (peri-somatic), and the other a slow (peri-dendritic) inhibitory population. In the same study, it was shown that the addition of the peri-somatic inhibitory population made it possible for the neural mass model to replicate the key characteristics of low amplitude high frequency EEG. This model is referred to as the neural mass model of the hippocampus.

This model is capable of replicating key characteristics observed in EEG prior to and during seizure.

The neural mass model of the hippocampus is capable of replicating key features observed in EEG prior to, during and post seizure. The model can replicate key features by altering parameters that describe the balance between excitation and inhibition in the modeled region of the brain. The model, although it is described in a neuronal sense, is not a model of the brain. However, it is a good descriptor of EEG recorded from the hippocampus. Due to its description of neuronal connections and systems in terms of populations the model is relatively uncomplicated. This is shown in Wendling et al. (2002) where key features observed prior to, during and post seizure can all be replicated by altering three model parameters, which describe the balance between excitation and inhibition. This ability of the model means that only three model parameters need to be estimated, and allow imaging of these unmeasured dynamics using estimation.

Previous work on estimating the neural mass model of the hippocampus has been done using a genetic algorithm.

The neural mass model of the hippocampus has previously been estimated using the genetic algorithm (Wendling et al., 2005). The genetic algorithm is capable of estimating model parameters using recursion. This makes the method accurate but time consuming. Therefore, results from studies using the genetic algorithm are often limited. The result of which is incomplete characterisation of EEG, with little to no evidence of the changes in model parameters observed during the transitions from normal to ictal EEG being unique.

What is being done, and why is it better or different?

In this paper, the accuracy of estimating the three model parameters describing the balance between excitation and inhibition using an unscented Kalman filter is determined. In order to achieve

this, artificial EEG is simulated using the neural mass model of the hippocampus. The artificial EEG is then considered to be the observations in the estimation procedure. Model parameters are then estimated, under the assumption that they were originally unknown.

Why the Kalman filter The filter, unlike the genetic algorithm, does not rely on recursion and is therefore less time consuming. This comes at the cost of accuracy. This paper looks at the accuracy of the filter under numerous conditions to determine how robust it is. If the unscented Kalman filter is accurate at estimating model parameters then this method could be used further to help characterise full EEG data sets, and allow for treatments to be evaluated and developed.

Structure of the paper In the methods section, a description of the neural mass model of the hippocampus is presented, as well as the equations used to simulate the model. Further, the formulation of the unscented Kalman filter for the neural mass model of the hippocampus is described. In the results section, the performance of the algorithm under numerous conditions are demonstrated. Lastly, in the discussion an evaluation of the performance of the filter is provided, discussing whether this method is a viable way forward to use model estimation to help image the effect that disorders and treatments have on the brain.

2 Methods

What we are doing in this paper The Wendling model is capable of replicating key features of observed in hippocampal EEG prior to, during and post seizure (Wendling et al., 2002). Here the estimation of physiologically relevant model parameters from the Wendling model is considered. An unscented Kalman filter is used to estimate the model parameters of interest. For this study the estimation procedure is tested using artificial EEG simulated using the Wendling model. By doing so it is possible to determine how robust the unscented Kalman filter is when estimating the Wendling model.

2.1 Model Description and Simulation

Wendling model description.

The Wendling model describes the aggregate membrane potentials and firing rates produced by different neural populations. The populations are then excited or inhibited by other populations in the model. The net effect of one population on another is determined by a scaling constant termed the connectivity constant. A graphical representation of the model is shown in Figure 1. In the model four different neural populations are considered. The pyramidal neural population is the generator of the model output, and its aggregate membrane potential is the simulated artificial EEG. Excitatory interneurons excite the pyramidal neurons. Slow and fast inhibitory interneurons inhibit the pyramidal neural population. Further, the pyramidal neural population excites the excitatory, slow and fast inhibitory populations. Lastly, slow inhibitory interneurons inhibit the fast inhibitory neural population. The effect of each neural population on the other is scaled by a connectivity constant. This connectivity constant accounts for the number of neurons within each population. Lastly, a stochastic input to the model is added to account for the effect of afferent pyramidal neurons on the modeled neural mass.

Mathematical functions used in the model The Wendling model consists of two primary structures. The first structure is a sigmoid function which converts an aggregate membrane potential to an average firing rate (Equation 1). In equation 1 $g(v(t))$ is the firing rate, g_{max} is the maximum firing rate, r is the sigmoid gradient and v_0 is the membrane potential at which $0.5g_{max}$ is reached. The second structure is an average firing rate to aggregate membrane potential kernel (Equations 2-3). In equations 2-3 $v_k(t)$ is the aggregate membrane potential, $h_k(t)$ is kernel which converts firing rates into membrane potentials, $\theta_k(t)$ is the synaptic gain and τ_k is the time

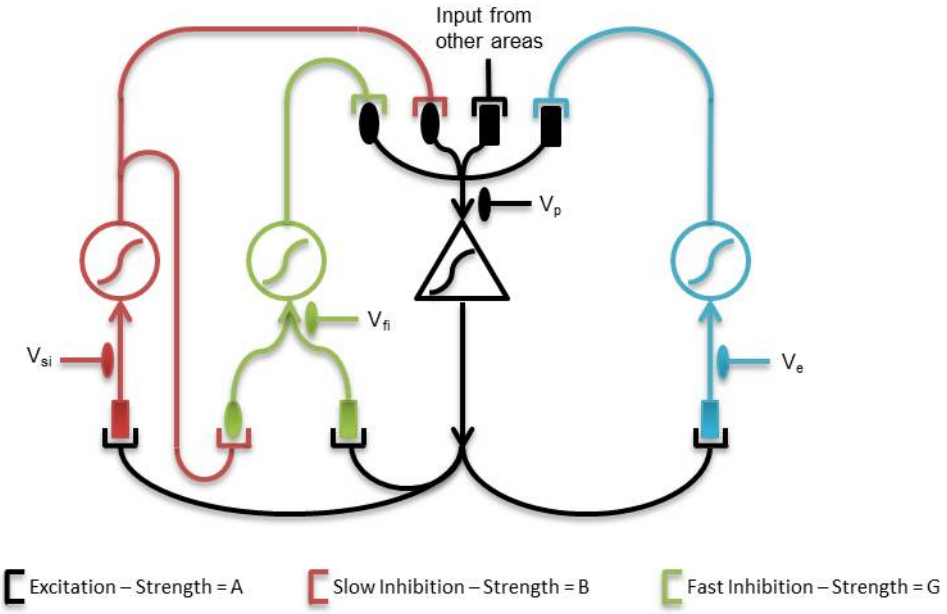

Figure 1: Graphical Descption of the Wendling model.

constant. $h_k(t)$ is a delayed exponential decay function (Figure 2).

$$g(v(t)) = \frac{g_{max}}{1 + exp(r(v(t) - v_0))} \tag{1}$$

$$v_k(t) = h_k(t) * g(v(t)) \tag{2}$$

$$h_k(t) = \frac{\theta_k(t)}{\tau_k} texp\left(-\frac{t}{\tau_k}\right). \tag{3}$$

Here the subscript k is used to indicate that each neural population is described with a different synaptic gain and time constant. The synaptic gains are described by θ_k as they are the parameters that are altered in order to simulate artificial seizure EEG (Figure 3). Further, the synaptic gains will be the variables that are estimated in this study. In this description of the Wendling model numerous model parameters are considered to be stationary, this includes the maximum firing rate (g_{max}) and time constants (τ_k). Equations 2-3 can be converted into a set of two differential equations

$$\dot{v}_k(t) = z_k(t) \tag{4}$$

$$\dot{z}_k(t) = \frac{\theta_k(t)}{\tau_k} n_k u_k(t) - 2\frac{z_k(t)}{\tau_k} - \frac{v_k(t)}{\tau_k^2}. \tag{5}$$

Here $v_k(t)$ is the average membrane potential and $z_k(t)$ is its derivative. $\theta_k(t)$ and τ_k are the specific neural populations synaptic gain and time constant. Lastly, $u_k(t)$ is the firing rate to the specific neural population considered and n_k is a constant used to specify connectivity.

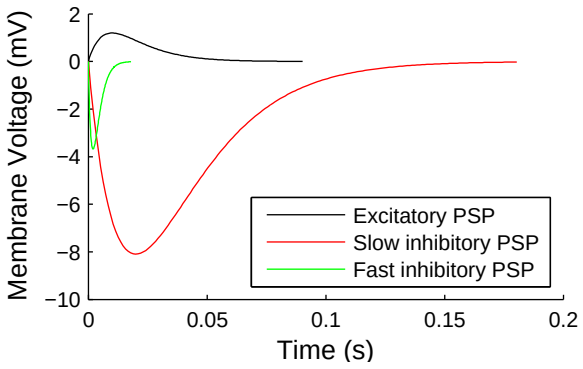

Figure 2: Firing rate to aggregate membrane potential converter.

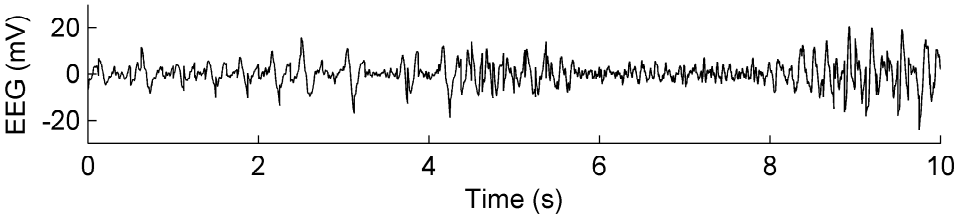

Figure 3: Artificial seizure simulated using the wendling model.

Full mathematical description of the model Using equations 4-5 the model can be described by a set of eight stochastic differential equations

$$dv_{po}(t) = z_{po}(t)dt \tag{6}$$

$$dz_{po}(t) = \left(\frac{\theta_p(t)}{\tau_p} n_p g(v_p(t)) - 2\frac{z_{po}(t)}{\tau_p} - \frac{v_{po}(t)}{\tau_p^2}\right) dt \tag{7}$$

$$dv_{eo}(t) = z_{eo}(t)dt \tag{8}$$

$$dz_{eo}(t) = \left(\frac{\theta_e(t)}{\tau_e}(\mu + n_e g(v_e(t)) - 2\frac{z_{eo}(t)}{\tau_e} - \frac{v_{eo}(t)}{\tau_e^2}\right) dt + \frac{\theta_e(t)}{\tau_e}\epsilon(t)dW \tag{9}$$

$$dv_{sio}(t) = z_{sio}(t)dt \tag{10}$$

$$dz_{sio}(t) = \left(\frac{\theta_{si}(t)}{\tau_{si}} n_{si} g(v_{si}(t)) - 2\frac{z_{sio}(t)}{\tau_{si}} - \frac{v_{sio}(t)}{\tau_{si}^2}\right) dt \tag{11}$$

$$dv_{fio}(t) = z_{fio}(t)dt \tag{12}$$

$$dz_{fio}(t) = \left(\frac{\theta_{fi}(t)}{\tau_{fi}} n_{fi} g(v_{fi}(t)) - 2\frac{z_{fio}(t)}{\tau_{fi}} - \frac{v_{fio}(t)}{\tau_{fi}^2}\right) dt. \tag{13}$$

dW represents a Wiener process and is required as $\epsilon(t) \longmapsto N(0, \sigma)$. Here σ and μ describe the mean and variance of the stochastic model input. Further, $v_{ko}(t)$ and $z_{ko}(t)$ represent the membrane potential produced by each neural population. $v_k(t)$ and $z_k(t)$ are the inputs to each neural population, and are considered to be the membrane potential of the specific population. k

takes the values of p, e, fi and si representing pyramidal, excitatory, and slow and fast inhibitory populations, respectively. Therefore $v_p(t)$ is the output of the model. All $v_k(t)$ can be described in terms of $v_{ko}(t)$ as follows

$$v_p(t) = v_{eo}(t) - v_{sio}(t) - v_{fio}(t) \tag{14}$$

$$v_e(t) = c_1 v_{po}(t) \tag{15}$$

$$v_{si}(t) = c_3 v_{po}(t) \tag{16}$$

$$v_{fi}(t) = c_5 v_{po}(t) - c_6 v_{sio}(t), \tag{17}$$

where c_1, c_3 and c_5 represent the connectivity strength from pyramidal to excitatory, slow inhibitory and fast inhibitory populations, respectively. c_6 represents the connectivity strength from the slow to the fast inhibitory population. Lastly, all n_k can be defined as connectivity constants

$$n_p = 1 \tag{18}$$

$$n_e = c_2 \tag{19}$$

$$n_{si} = c_4 \tag{20}$$

$$n_{fi} = c_7. \tag{21}$$

Here c_2, c_4 and c_7 represent the connectivity strength from excitatory, slow inhibitory and fast inhibitory to the pyramidal population.

Simulation of model This set of continuous stochastic differential equations is discretised using Euler-Mariyama's method, to simulate the artificial EEG.

$$v_{po,t+T} = v_{po,t} + T z_{po,t} \tag{22}$$

$$z_{po,t+T} = z_{po,t} + T\left(\frac{\theta_{p,t}}{\tau_p} n_p g(v_{p,t}) - 2\frac{z_{po,t}}{\tau_p} - \frac{v_{po,t}}{\tau_p^2}\right) \tag{23}$$

$$v_{eo,t+T} = v_{eo,t} + T z_{eo,t} \tag{24}$$

$$z_{eo,t+T} = z_{eo,t} + T\left(\frac{\theta_{e,t}}{\tau_e}(\mu + n_e g(v_{e,t}) - 2\frac{z_{eo,t}}{\tau_e} - \frac{v_{eo,t}}{\tau_e^2}\right) + \sqrt{T}\frac{\theta_{e,t}}{\tau_e}\epsilon_t \tag{25}$$

$$v_{sio,t+T} = v_{sio,t} + T z_{sio,t} \tag{26}$$

$$z_{sio,t+T} = z_{sio,t} + T\left(\frac{\theta_{si,t}}{\tau_{si}} n_{si} g(v_{si,t}) - 2\frac{z_{sio,t}}{\tau_{si}} - \frac{v_{sio,t}}{\tau_{si}^2}\right) \tag{27}$$

$$v_{fio,t+T} = v_{fio,t} + T z_{fio,t} \tag{28}$$

$$z_{fio,t+T} = z_{fio,t} + T\left(\frac{\theta_{fi,t}}{\tau_{fi}} n_{fi} g(v_{fi,t}) - 2\frac{z_{fio,t}}{\tau_{fi}} - \frac{v_{fio,t}}{\tau_{fi}^2}\right). \tag{29}$$

Table 1: Static Model Parameters

Model parameter	Physical description	Value	Units
τ_p	Time constant for pyramidal neurons	100	s^{-1}
τ_e	Time constant for excitatory neurons	100	s^{-1}
τ_{si}	Time constant for slow inhibitory neurons	35	s^{-1}
τ_{fi}	Time constant for fast inhibitory neurons	500	s^{-1}
c	Connectivity constant	135	NA
g_{max}	Maximum firing rate	5	Hz
v_0	PSP for which 50% firing rate is achieved	6	mV^{-1}
r	Gradient of sigmoid function	0.56	NA
μ	Input mean firing rate	90	Hz
σ	Variance of input firing rate	15	Hz

Table 2: Static model parameters: Connectivity. C is the connectivity constant specified in Table 1. Terms in brackets indicate the direction in which the constant affects the system. Here P, E, SI and FI represent populations of pyramidal neurons and excitatory, slow inhibitory and fast inhibitory interneurons, respectively.

Model parameter	Physical description	Value
c_1	Connectivity constant (P - E)	C
c_2	Connectivity constant (E + I - P)	$0.8C$
c_3	Connectivity constant (P - SI)	$0.25C$
c_4	Connectivity constant (SI - P)	$0.25C$
c_5	Connectivity constant (P - FI)	$0.3C$
c_6	Connectivity constant (SI - FI)	$0.1C$
c_7	Connectivity constant (SI - P)	$0.8C$

Here T is the period between solutions. The static parameter values are demonstrated in Tables 1-2. The variance of the input (σ) is specified such that 99.7% of realisations drawn from the Gaussian distribution fall within the specified maximum and minimum firing rate. In this case, the firing rate limits are set to 30 and 150. For the cases where the realisations from the Gaussian distribution are not contained within the limits specified, the specific sample of interest is redrawn from the same Gaussain distribution until the firing rate falls within the specified range. In Table 1 the parameters $\theta_{p,t}$, $\theta_{e,t}$, $\theta_{si,t}$ and $\theta_{fi,t}$ are not specified as these parameters will vary for different simulations. However,for this simulation it is assumed that

$$\theta_{p,t} = \theta_{e,t}. \tag{30}$$

2.2 Estimation

Generic description on a nonlinear system To begin we define a generic nonlinear system where

$$\dot{\mathbf{x}}(t) = \mathbf{A}(\mathbf{x}(t), \theta(t)) + \mathbf{B}(\mathbf{u}(t)) + \mathbf{n}(t)\mathbf{y}(t) = \mathbf{C}(\mathbf{x}(t)) + \mathbf{r}(t), \tag{31}$$

with $x(t)$ the state vector and $\dot{x}(t)$ its derivative where

$$\dot{x}(t) = \begin{bmatrix} \dot{x}_1(t) \\ \vdots \\ \dot{x}_n(t) \end{bmatrix}.$$

$\mathbf{A}$, $\mathbf{B}$ and $\mathbf{C}$ are the state, input and output matrices and $u(t)$ the input to the model. $\mathbf{y}(t)$ is the model output with $\mathbf{n}(t)$ the model noise, or uncertainty and $\mathbf{r}(t)$ the measurement error, or observation noise. Here $\mathbf{n}(t)$ takes into account that the model is not a perfect descriptor of the particular region of the brain, and $\mathbf{r}(t)$ describes the maximum amplitude of the noise in the observations. Both $\mathbf{n}(t)$ and $\mathbf{r}(t)$ are zero mean Gaussian distributions with a system dependant variance. It is important to note that this assumption of a Gaussian distribution is only valid when the number of samples for the estimation procedure is large.

Introduction to the UKF Estimation is usually performed to estimate the model states $x(t)$ given some observation $y(t)$. One method that is often use for estimation linear systems in the Kalman filter. The Kalman filter consists of two steps: prediction and correction. In the prediction step model states are propagated through the system in order to give an estimate of the expected value of the states at the next time step. Using a first order Euler-Maruyama method this can be described by

$$\mathbf{x}^-_{t+T} = \mathbf{x}_t + T\mathbf{A}(\mathbf{x}_t) + \sqrt{T}\mathbf{n}_t\mathbf{y}^-_{t+T} = \mathbf{y}_t + T\mathbf{C}(\mathbf{y}_t) + \sqrt{T}\mathbf{r}_t \tag{32}$$

where the subscript in x^-_t is used to indicate a discrete time description and T is the sampling period. The superscript in x^-_t is used to indicate that this estimate is a prediction that has not yet been corrected by the current observation. Performing this kind of prediction for a nonlinear system would be inaccurate. The reason for this is that propagation of states like this in a system would require the assumption that the error in the states remains constant for all time. However, in a nonlinear system this is not true, as states error can vary drastically across time steps. In other words if the original state estimate is incorrect in a nonlinear system it is possible that the error can increase from one step to the next, which is not the case for linear system. In order to account for this error, or state covariance changing an unscented filter is used in the prediction step for nonlinear systems. The advantage of an unscented filter over local linearisation techniques is both speed is improved and discontinuities can still be modeled.

The unscented filter The unscented filter is completely described by the states mean and covariance such that we can draw sigma points that are defined as

$$\S_n = \overline{\mathbf{x}}_t + (\sqrt{\kappa + D_x\mathbf{P}_{\mathbf{xx,t}}})_n \quad n = 1, \ldots, D_x \tag{33}$$

$$\S_{n+D_x} = \overline{\mathbf{x}}_t - (\sqrt{\kappa + D_x\mathbf{P}_{\mathbf{xx,t}}})_n \quad n = 1, \ldots, D_x, \tag{34}$$

where $\overline{\mathbf{x}}_t$ is the current state estimate. $\sqrt{\cdot}_n$ denotes the nth row or column of the matrix square root. D_x is the number of states in the system and $\mathbf{P}_{\mathbf{xx,t}}$ is the covariance matrix or expected error of the current state estimate. κ is a predefined constant which determine the relative effect of the propagation of the mean. For now if κ is equal to zero than the system mean is not propagated as a sigma point. However, if κ is greater than zero then

$$\mathcal{X}_0 = \overline{\mathbf{x}}_t. \tag{35}$$

Now their are $2D_x$ sigma points when κ is zero or $2D_x$+1 sigma points when it is greater than zero. These sigma points are then propagated through the system in oder to update the expectation about the state mean and error.

$$\S_{n,t+T} = \S_t + T\mathbf{A}(\S_{n,t}) + \sqrt{T}n_t \tag{36}$$

$$\overline{\mathbf{x}}^-_{t+T} = \frac{1}{2D_x + \kappa}\sum_{n=1}^{2D_x} \S_{n,t+T} \tag{37}$$

$$\mathbf{P}^-_{xx,t+T} = \frac{1}{2D_x + \kappa}\sum_{n=1}^{2D_x} (\S_{n,t+T} - \overline{\mathbf{x}}^-_{t+T})(\S_{n,t+T} - \overline{\mathbf{x}}^-_{t+T})^\top \mathbf{Q}. \tag{38}$$

Here $\overline{\mathbf{x}}^{-}_{t+T}$ and $\mathbf{P}^{-}_{xx,t+T}$ are the predictions for the state and state covariance matrices. The superscript a^{-} is used to indicate an uncorrected prediction. $\mathbf{Q}$ is the expectation of the model error n_t. Further, it is possible to make a prediction about the observation at time $t+T$ by propagating the sigma points through equation 32

$$\dagger_{n,t+T} = \dagger_t + T\mathbf{C}(\S_{n,t}) + \sqrt{T}r_t \tag{39}$$

$$\overline{\mathbf{y}}^{-}_{t+T} = \frac{1}{2D_x+\kappa}\sum_{n=1}^{2D_x}\dagger_{n,t+T} \tag{40}$$

$$\mathbf{P}^{-}_{xy,t+T} = \frac{1}{2D_x+\kappa}\sum_{n=1}^{2D_x}(\S_{n,t+T}-\mathbf{x}_{n,t+T})(\dagger_{n,t+T}-\overline{\mathbf{y}}^{-}_{t+T})^{\top} \tag{41}$$

$$\mathbf{P}^{-}_{yy,t+T} = \frac{1}{2D_x+\kappa}\sum_{n=1}^{2D_x}(\dagger_{n,t+T}-\overline{\mathbf{y}}^{-}_{t+T})(\dagger_{n,t+T}-\overline{\mathbf{y}}^{-}_{t+T})^{\top}+\mathbf{R}, \tag{42}$$

where $\overline{\mathbf{y}}^{-}_{t+T}$ and $\mathbf{P}^{-}_{yy,t+T}$ are the predictions for the model output and its covariance. $\mathbf{P}^{-}_{xy,t+T}$ is the covariance matrix of the states and observations. Lastly, $\mathbf{R}$ is the expectation of the observation error r_t.

How states are predicted using the unscented transform The predictions of the states ($\overline{\mathbf{x}}^{-}_{t+T}$) and observations ($\overline{\mathbf{y}}^{-}_{t+T}$) now need to be corrected based on the observations. This is achieved by

$$\mathbf{K} = \mathbf{P}^{-}_{xy,t+T}(\mathbf{P}^{-}_{yy,t+T})^{-1} \tag{43}$$

$$\mathbf{x}_{t+T} = \overline{\mathbf{x}}^{-}_{t+T} + \mathbf{K}(\mathbf{y}_{t+T}-\overline{\mathbf{y}}^{-}_{t+T}) \tag{44}$$

$$\mathbf{P}_{xx,t+T} = \mathbf{P}^{-}_{xx,t+T} - \mathbf{K}(\mathbf{P}^{-}_{xy,t+T})^{\top}, \tag{45}$$

where $\mathbf{y}_t$ is the recording or observation made, $\mathbf{x}_{t+T}$ is estimate of the state and $\mathbf{P}_{xx,t+T}$ is the estimate of the error on the state. This set of equations describes the UKF and how it can be used to estimate states. However, for this study estimation of states and parameters needs to be achieved (dual estimation).

Definition of slow state matrix and its dynamics Firstly, reconsider the extended neural mass model. The parameters that are being estimated are θ_p, θ_e, θ_{si} and θ_{fi}. Here it is assumed that

$$\theta_p = \theta_e. \tag{46}$$

Therefore, three parameters need to be estimated, and a parameter matrix is defined

$$\theta_t = \begin{bmatrix} \theta_{p,t} \\ \theta_{si,t} \\ \theta_{fi,t} \end{bmatrix}.$$

This parameter matrix is then augmented to the original state matrix

$$\mathbf{x}_t = \begin{bmatrix} \mathbf{x}_t \\ \theta_t \end{bmatrix}.$$

Note that parameters will now be referred to as slow states, to allow for ease of reference to the newly defined state matrix. The next issue to consider is the description of the dynamics for the slow states. Due to the prediction correction steps of the unscented Kalman filter these slow states can be assigned trivial dynamics such that

$$\theta_{t+T} = \theta_t + \eta_{\mathbf{t}} \tag{47}$$

$$E(\theta_{t+T}) = \theta_t \tag{48}$$

$$P_{\theta\theta,\mathbf{t+T}} = \mathbf{\Psi}, \tag{49}$$

where $E(\cdot)$ is the expectation function and $\eta_t \longmapsto N(0,\sigma)$.

Intialisation of UKF for stationary parameters When initialising the unscented Kalman filter the uncertainty and standard deviation of the model needs to be specified. Initial estimations are performed under the assumption that the model's slow states are stationary. This assumption allows the uncertainty in slow states to be minimal. The reason for this being that this uncertainty in this case describes only model inaccuracy and not the trivial dynamics of the slow states. Standard deviations in the estimation description are described such that one standard deviation from the midpoint of the specified states range encompasses all possible values for the particular state. Further to this the uncertainty of states directly affected by the stochastic model input is increased to account for the randomness of this signal

when simulating. This is required as a stochastic process such as this cannot, at present, be estimated accurately.

Intialisation of UKF for varying parameters Secondly, estimation of varying slow states required the addition of the trivial dynamics described in equation 47. It is assumed that the uncertianty of the model error and slow state dynamics are additive.

Estimation of model input mean Lastly, estimation of the stochastic inputs mean to the neural mass is considered. In order to achieve this it is assumed that the model input mean can be assumed to be varying slowly, similarly to the model's slow states. By doing so the input mean can be augmented to the state matrix and assigned trivial dynamics.

UKF estimation bounds and initialsation of states When performing estimation, the results on the model's slow states are bounded by their physiological range as specified by Wendling et al. (2002). Further, the initial estimate of the model states is described as a Gaussian with the mean specified as the midpoint of the states range and the standard deviation set such that 99.9% of realisations are within the specified physiolgical range of the specific state.

Robustness test To determine how robust the estimation procedure is the effect of noise and varying initialisations of the model states are considered. Further, the ability of the estimation procedure to estimate varying slow states, with different rates of change is determined.

References

Freeman, W. (1963). The electrical activity of a primary sensory cortex: analysis of eeg waves. *Int. Rev. Neurobiol*, 5:53–119.

Jansen, B. and Rit, V. (1995). Electroencephalogram and visual evoked potential generation in a mathematical model of coupled cortical columns. *Biological Cybernetics*, 73(4):357–366.

Lopes da Silva, F., Hoeks, A., Smits, H., and Zetterberg, L. (1974). Model of brain rhythmic activity. *Biological Cybernetics*, 15(1):27–37.

Voss, H., Timmer, J., and Kurths, J. (2004). Nonlinear dynamical system identification from uncertain and indirect measurements. *International Journal of Bifurcation and Chaos*, 14(6):1905–1933.

Wendling, F., Bartolomei, F., Bellanger, J., and Chauvel, P. (2002). Epileptic fast activity can be explained by a model of impaired GABAergic dendritic inhibition. *European Journal of Neuroscience*, 15(9):1499–1508.

Wendling, F., Hernandez, A., Bellanger, J., Chauvel, P., and Bartolomei, F. (2005). Interictal to ictal transition in human temporal lobe epilepsy: Insights from a computational model of intracerebral EEG. *Journal of Clinical Neurophysiology*, 22(5):343.

White, J., Banks, M., Pearce, R., and Kopell, N. (2000). Networks of interneurons with fast and slow γ-aminobutyric acid type a (gabaa) kinetics provide substrate for mixed gamma-theta rhythm. *Proceedings of the National Academy of Sciences*, 97(14):8128.